

Understanding the effect of counterpressure buildup during syringe injections

Md Shahriar¹, Ankit Rewanwar¹, Pankaj Rohilla¹, Jeremy Marston*

Department of Chemical Engineering, Texas Tech University, Lubbock, TX 79409, United States

ARTICLE INFO

Keywords:
Injectability
Counter-pressure
Force
Rheology
Intradermal
intramuscular
Subcutaneous

ABSTRACT

The pain felt during injection, typically delivered via a hypodermic needle as a single bolus, is associated with the pressure build-up around the site of injection. It is hypothesized that this counterpressure is a function of the target tissue as well as fluid properties. Given that novel vaccines target different tissues (muscle, adipose, and skin) and can exhibit a wide range of fluid properties, we conducted a study of the effect of volumetric flow rate, needle size, viscosity and rheology of fluid, and hyaluronidase as an adjuvant on counterpressure build-up in porcine skin and muscle tissues. In particular, we found a significant increase in counterpressure for intradermal (ID) injections compared to intramuscular (IM) injections, by an order of magnitude in some cases. We also showed that the addition of adjuvant affected the tissue back pressure only in case of subcutaneous (SC) injections. We observed that the volumetric flow rate plays an important role along with the needle size. This study aims to improve the current understanding and limitations of liquid injectability via hypodermic needles, however, the results also have implications for other technologies, such as intradermal jet injection where a liquid bleb is formed under the skin.

1. Introduction

The design and development of various injection devices for liquid drug delivery requires consideration of user capability and forces that contribute to the drug administration process (Allmendinger et al., 2014). Transdermal drug delivery is one of the common methods of drug administration, including intradermal, subcutaneous and intramuscular regions (Yildiz and Lenau, 2019). Drug delivery into the intramuscular and subcutaneous regions has shown some advantages over intravenous delivery, such as easier drug administration and sustained absorption rate (Shrestha and Stoeber, 2018; Kim et al., 2017; Richter et al., 2012; McDonald et al., 2010; Harris et al., 2004; Pivot et al., 2013), while intradermal injection of some vaccines can generate an equivalent or better immune response than intramuscular injection with a reduced dosage (Saitoh and Aizawa, 2016; Wangmo et al., 2019). Muscular regions are comprised of muscle tissues with rich blood supply in comparison to intradermal and subcutaneous regions (Salari et al., 2018; Wynaden et al., 2015), therefore drugs which require quick absorption with a sustainable action, as well as concentrated and irritant drugs which can not be given intradermally or intravenously, are generally

targeted for intramuscular delivery (Tuğrul and Khorshid, 2014).

However, whether it is for subcutaneous or intramuscular injections, the injector must overcome different characteristic forces which depend on the geometry of the injector and the liquid properties of the injectate (Yildiz and Lenau, 2019; Allmendinger et al., 2015). Parameters related to the device including syringe diameter (d_s), needle inner diameter (d_i), and needle length (L_n) play an important role in the hydrodynamic component of the injection forces. The other parameters related to injection forces are human factors, drug properties which depend on the temperature and drug concentration (Allmendinger et al., 2014; Allmendinger et al., 2015; Rathore et al., 2012; Burckbuchler et al., 2010), and friction between the plunger material and the syringe barrel. To characterize the syringe performance, three forces have been evaluated (Pstras, 2016; Lorenz et al., 2013): Break-loose force (F_B), i.e., the force required to overcome the static friction to initiate the plunger motion and the forces measured at 50% and 99.9% delivery of the total target volume. According to Lorenz et al. (2013), the design of the plunger stopper, materials of the barrel and plunger, and environmental conditions such as temperature and humidity contribute to kinetic friction. Whereas, static friction depends on the time of stationary contact and

* Corresponding author.

E-mail address: jeremy.marston@ttu.edu (J. Marston).

¹ Equal contribution.

the properties of the plunger and barrel material (Lorenz et al., 2013). Generally, static friction is larger than the kinetic friction in syringes and other injection systems (Pstras, 2016).

Furthermore, it is important to understand the counterpressure during injection to facilitate painless administration of the drug with improvement in user friendliness (Yildiz and Lenau, 2019). As per a recent study on subcutaneous injections in human subjects, tissue counterpressure was observed to increase with an increase in the infusion rate (Patte et al., 2013) suggesting a limit on how fast liquid can diffuse out from the injection site. In another study, Cilurzo et al. (2011) observed that the characteristic forces such as break-loose force, gliding force, and maximum measured force (F_{max}) during SC injection into human tissue depend on the dimensions of the needle syringe used in addition to the viscosity of the solutions used. Multiple studies have been conducted on the measurement of tissue back pressure with variation in infusion rate and drug properties during *in vivo* and *ex vivo* injections targeted to SC and ID regions (Allmendinger et al., 2015; Thomsen et al., 2014; Vosseler et al., 2011). These studies highlighted the importance of considering targeted regions before the selection of optimal diameter and length of needles, and the role of permeability and bulk modulus of the tissue on the counter-pressure.

Adjuvants such as hyaluronidase facilitate the diffusion capability and bioavailability of the injected drugs (Buhren et al., 2016; Meyer, 1947). Hyaluronidases are a family of enzymes that disaggregate and depolymerize hyaluronic acid (HA), commonly found in the dermis. Due to its extremely hydrophilic nature, HA has a very high hydration capacity which supports the viscoelastic nature of the skin, and it also plays a vital role as a lubricant and shock absorber (Buhren et al., 2016; Meyer, 1947). Upon depolymerization of HA, its viscosity and lubrication properties decrease (Cavallini et al., 2013). Thus, when used as an adjuvant, hyaluronidase helps in diffusion and bioavailability of the injected drugs. Owing to such properties of this enzyme, it is used therapeutically to increase the absorption rate of drugs as well as lessen the discomfort associated with subcutaneous and intramuscular injections (El-Safory et al., 2010).

Although multiple studies have been conducted to measure the counterpressure in the tissue during injection into intradermal and subcutaneous regions (Kim et al., 2017; Allmendinger et al., 2015; Comley and Fleck, 2011; Thomsen et al., 2015; Leuenberger et al., 2013), counterpressure buildup in intramuscular regions is poorly understood. In addition, the effect of variation in force measurements due to the inherent properties of the syringe has not been considered before. In this study, we measure the force profile during injection of liquids with different viscosity and rheology into air (as reference) and then into intradermal, subcutaneous, and intramuscular regions of porcine skin. We also studied the variation in force measurements for single and multiple usage of syringes to identify a range of trials for minimum intrasample variation due to syringe properties, in order to eliminate the effect of the syringe as a source of variation in the experiments. In this range, liquids were injected in air and into the skin (*or muscle tissue*) alternatively for 5 trials each. The difference of these forces yields the net force indicating the effect of tissue counterpressure. The characteristic forces measured herein were: (i) break-loose force (F_B), (ii) force measured at 50% delivery of the liquid ($F_{50\%}$) and (iii) force measured at 99.9% liquid delivery ($F_{99.9\%}$). Different concentrations of glycerol and CMC solutions were used to study the effect of rheology on the counterpressure buildup. The volumetric flow rate, target volume, and needle size were also varied to understand their effect on counterpressure buildup within the tissue.

2. Materials and methods

2.1. Materials

DI water and glycerol solutions in different concentrations (50%, 80%, and 95% w/w) were used as Newtonian liquids and Sodium car-

boxymethyl cellulose (CMC, *average molecular weight* $\approx 7 \times 10^5$, Sigma-Aldrich) solutions in different concentrations (0.125%, 0.25%, 0.5%, 1%, and 2% w/w) were used as non-Newtonian liquids. Trypan blue (Sigma Aldrich) was added as a dye to these solutions in a concentration of 1 mg/ml to aid visualization of drug dispersion in tissue. These fluids were injected in different regions of skin via a needle attached to a 1 ml Luer-Lock BD syringe with the help of a syringe pump (KD Scientific, Legato-100).

2.2. Rheological measurements

Rheological measurements of the solutions were conducted on a DHR-2 rheometer (TA instruments) equipped with a cone and plate geometry ($\phi = 25$ mm and $\angle = 1.992^\circ$). A stress-controlled flow ramp was used to measure the flow behavior of the samples with a shear rate ($\dot{\gamma}$) ranging from 0.01 to 8,600 s⁻¹ for a time duration of 60 s at 22.8±0.2°C. Viscosities of the Newtonian liquids used in the study are presented in Table 1.

For non-Newtonian liquids, apparent viscosity was used. The apparent viscosity is a function of shear rate, $\dot{\gamma}$, which was calculated using:

$$\dot{\gamma} = \frac{4Q}{\pi R^3} \quad (1)$$

where Q is the volumetric flow rate of the liquid and R is the radius of the needle. The internal diameter ($D = 2R$) for 22 gauge (G), 25G, and 27G needles were 0.413 mm, 0.26 mm, and 0.21 mm, respectively.

The apparent viscosity (μ) at a shear rate of $\dot{\gamma}$ can be written using the Cross model relation as (Rohilla et al., 2019; Cross, 1965):

$$\mu_a = \mu_\infty + \left(\frac{\mu_0 - \mu_\infty}{1 + (\lambda \dot{\gamma})^n} \right) \quad (2)$$

where λ is a parameter with units of time, n is the dimensionless rate index parameter, μ_0 and μ_∞ represent values of asymptotic plateaus at $\dot{\gamma} \rightarrow 0$ and $\dot{\gamma} \rightarrow \infty$, respectively and are tabulated in supplementary info. Fitting to Eq. (2) yielded a range of apparent viscosities, given in Table 2 (across a suitable range of $\dot{\gamma}$).

2.3. Syringe operation

Various commercial syringes of different brands with different volume capacity were tested before conducting a parametric study. Force profiles during injection were compared to check the variation in force profiles for single and multiple usage of syringes. Although a syringe should not be reused to avoid cross-contamination which can spread blood-borne diseases, we have reused the syringe in the trials of the lowest intrasample variation of force profiles to rule out the effect of changing the syringe on counter-pressure buildup.

1 ml BD plastic syringes showed the lowest variation in force profiles for repeated trials amongst different commercial syringes tested for single and multiple use of up to 50 trials. To know the number of trials that could be done by a syringe without any significant effect on the delivery performance, air and water injections were performed 50 times for different syringes. Each syringe was removed from a sealed pack. The static friction between the plunger and barrel in a new syringe could be very high (Thornton et al., 2016), which could be the reason of the high break-loose force and noise in the force profile. As more trials were done with a given syringe, the friction reduced and the plunger could move smoothly. At first, we performed 50 injection trials with the same

Table 1
Viscosities of the Newtonian liquids used.

	Water	50% G	80% G	95% G
μ (mPa.s)	1	6.9	84	482

Table 2

A range of apparent viscosities (μ_a , mPa.s) estimated for a given range of shear rates for non-Newtonian fluids used.

	0.125% CMC	0.25% CMC	0.5% CMC	1% CMC	2% CMC
$\mu_a (\dot{\gamma}: 241 \rightarrow 36,681 \text{ s}^{-1})$	61.2 → 49.0	76.1 → 51.2	135.3 → 56.5	312.7 → 59.8	1110.5 → 76.7

syringe at a flow rate of 1 ml/min with and without water as an injectate. An intrasample variation of ~ 23% was observed in the force profiles of these 50 trials. Furthermore, a range of 10 trials (16 ≤ n ≤ 25) was identified with a lower intrasample variation (~ 4%) and higher reproducibility for different syringes. As such, before each experiment with a new syringe, the plunger was moved 15 times by hand slowly, and then 10 trials of liquid injection were performed in the air and porcine skin/tissue alternatively for 5 trials each. A comparison of force profiles for different syringes and different flow rates is presented in the [supplementary info](#).

Whilst the viscous friction in the needle can contribute considerably to the overall force, we sought to reveal the true resistance just from the target tissue. As such, reference measurements were performed where the liquid is ejected in air. This reference force is then subtracted from the force reading for injections into real tissue, leaving the net force ($F_{\text{net}} = F_{\text{cell}} - F_{\text{air}}$) which represents the contribution from the tissue alone.

2.4. Ex vivo injections

Tenderloin porcine tissue was procured from a local vendor for IM injection, while porcine skin was harvested from Yorkshire-Cross pigs euthanized at 13 weeks of age for ID injections. The harvested porcine skin was stored in a freezer at -20°C and was thawed to room temperature before performing injections. Intramuscular injections were performed on the tenderloin porcine tissue at different locations separated by a distance of $2 \pm 1 \text{ cm}$ with needles of different sizes (22G, 25G, and 27G) placed perpendicular to the tissue as shown in Fig. 1(b). Whereas, injections in the dermal region were performed at an angle in range of 10° – 15° with a 27G needle. Subcutaneous injections were administered via a 25G needle inserted at an angle of ~ 45° . A load cell (50 lb, LLB-350, Futek) sandwiched in between the moving shaft block of the syringe pump and the flat tail of the plunger was used for the force measurement at a sample rate of 100 Hz. The load cell utilizes a metal foil strain gauge system, measuring the resistance, which corresponds to the applied load or force.

A solution of bovine serum albumin (0.01% w/w) and phosphate buffer saline (Intermountain Life Sciences) was prepared to solubilize hyaluronidase powder at concentrations of 1 mg/ml and 2 mg/ml.

2.5. Design of experiments

In this study, we used a general factorial design, primarily focusing on the parameters including injectate properties (fluid viscosity), target region (IM, SC, and ID), volumetric flow rate and needle size. We performed 5 repeat trials ($n = 5$) for every parametric point involved in this study. The volumetric flow rate was varied in a range of 0.1–2 ml/min for ID and IM injections. We used needles of three different sizes i.e., 22 G, 25G, and 27G.

3. Results and discussions

Different liquids were injected into the intradermal and intramuscular regions of porcine skin with 27-gauge and 22-gauge needles, respectively. Fig. 2 shows example dispersion patterns formed after dyed water injection into ID and IM regions. Due to the higher needle insertion depth for IM injection, the bolus depth (d_b) was ~ 1.4 cm for IM injections as compared to ID injections ($d_b \sim 0.15 \text{ cm}$). Injected liquid seeps into the hole created by the needle for IM injection as can be observed from Fig. 2. It should be noted that for IM injections, the top layer of porcine skin was removed to make it easy for 22G needle to puncture into the intramuscular tissue.

3.1. Effect of viscosity

Here, we studied the effect of counter-pressure buildup during injection of Newtonian and non-Newtonian liquids into the intradermal and intramuscular regions. Fig. 3 shows the force profiles for different liquids when injected into air, and intradermal and intramuscular regions. For intradermal injection, 0.1 ml of liquid was injected through a 27-gauge needle; while for IM injections, 0.5 ml of liquid was injected through a 22-gauge needle. The flow rate ($Q = 1 \text{ ml/min}$) was kept constant for the injection of different liquids into different target regions. Solid lines and dashed lines in Fig. 3 represent force profiles for non-Newtonian and Newtonian liquids, respectively.

Fig. 3(a) and 3(b) show the force profiles for injection via a 22-gauge needle into air and porcine tenderloin tissue, respectively. Amongst Newtonian liquids, the force profile was within a range of 0.5–1.0 N for water, 50% glycerol, and 80% glycerol. The highest viscosity solution (95% glycerol) exhibited a higher force, ~ 2.3 N for injections into air and ~ 2.5 N for injection into tenderloin tissue. In all cases for IM

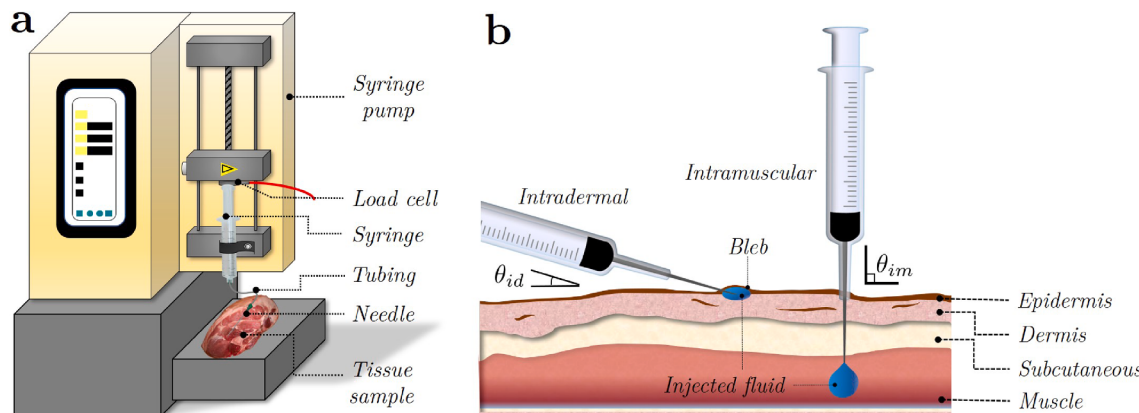


Fig. 1. Experimental (a) **schematics of experimental setup and (b)** **schematics showing intradermal and intramuscular injections into skin** ($\theta_{\text{id}} = 10^{\circ}$ – 15° and $\theta_{\text{im}} = 90^{\circ}$).

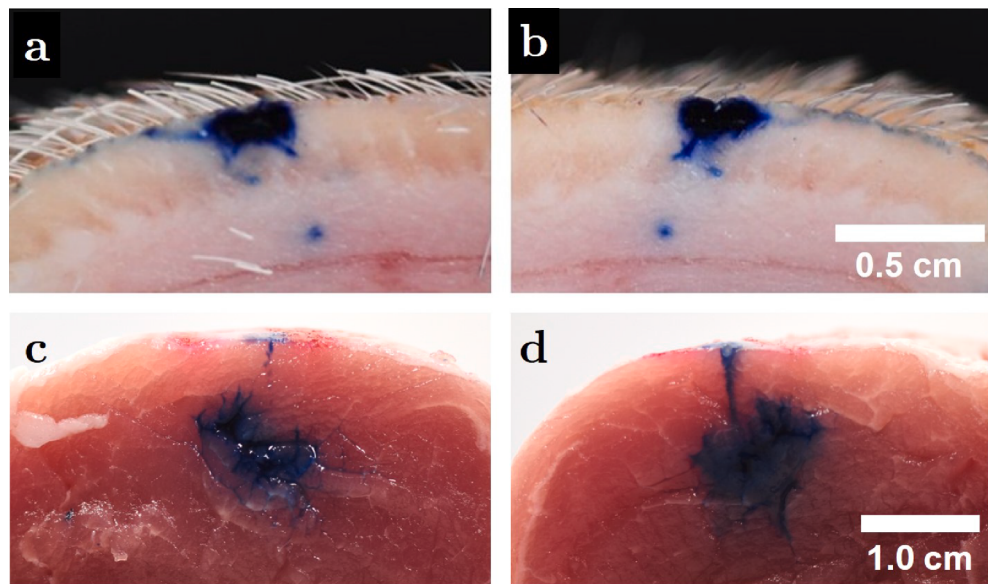


Fig. 2. Opposing views of injection sites. in (a,b) cross-sectional view of a skin bleb in the intradermal region of porcine skin ($V = 0.1 \text{ ml}$, 27 gauge needle, $Q = 1 \text{ ml/min}$), (c,d) cross-sectional view of intramuscular injection of dyed water in porcine tenderloin tissue ($V = 0.5 \text{ ml}$, 22 gauge needle, $Q = 1 \text{ ml/min}$).

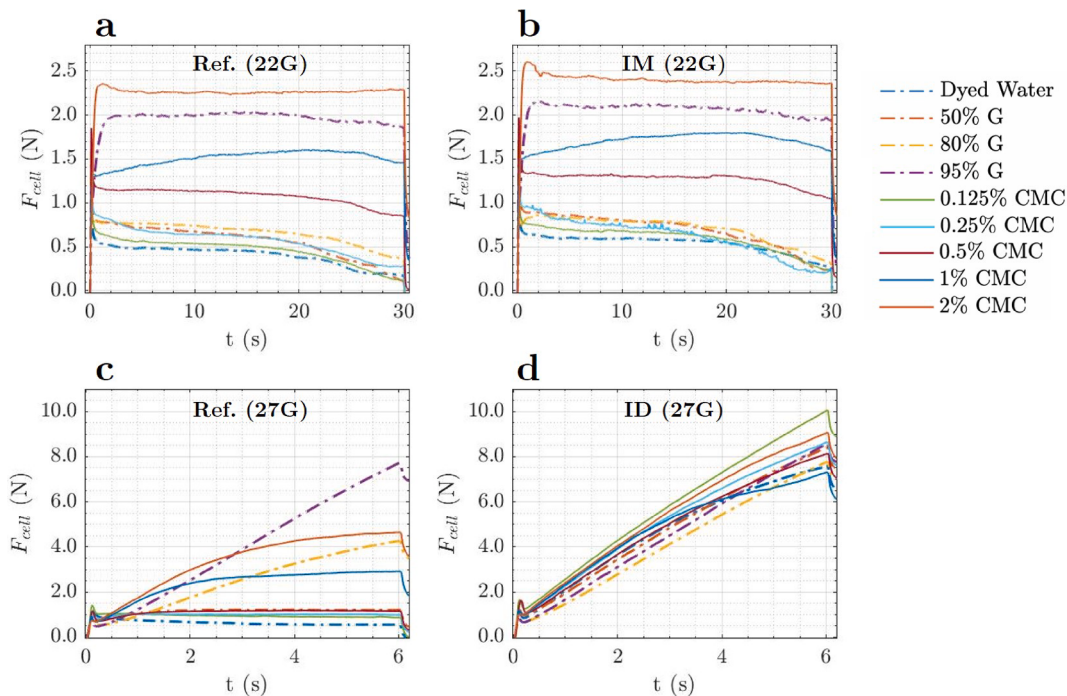


Fig. 3. Force profiles for injections with different liquids into (a) no target media i.e. expelled into air ($Q = 1 \text{ ml/min}$, $V = 0.5 \text{ ml}$, 22-gauge needle), (b) intramuscular region of porcine tenderloin tissue ($Q = 1 \text{ ml/min}$, $V = 0.5 \text{ ml}$, 22-gauge needle), (c) no target media i.e. expelled into air ($Q = 1 \text{ ml/min}$, $V = 0.1 \text{ ml}$, 27-gauge needle), and (d) intradermal injections ($Q = 1 \text{ ml/min}$, $V = 0.1 \text{ ml}$, 27-gauge needle).

injection via 22G needle, the force profile plateaued very quickly, whereas for the IM injections via 27G needle (fig 3(c,d)), a qualitatively different force profile was observed, especially for the high viscosity solutions.

In the case of injection into skin (ID), the force was much higher as a result of counter-pressure build-up during liquid inflow. In general, the target liquid volume for the intradermal region does not exceed 0.1 ml. Increasing the target volume in the intradermal region could lead to leaching of liquid beyond the dermis layer into the subcutaneous region, which is undesirable as the drugs are designed to be delivered into specific regions. The total force needed for intradermal injection

varied in the range of $\sim 0.5 \rightarrow 2.5 \text{ N}$, whereas for intradermal injection, the total force increased linearly from $\sim 1 \text{ N} \rightarrow 7\text{--}10 \text{ N}$, showing a significant increase due to both the finer gauge needle and increased tissue resistance.

Rheological characterization of CMC solutions (supplementary Fig. S1) showing change in apparent viscosity with applied shear rate were similar to that obtained in earlier studies (Rohilla et al., 2019; Benchabane and Bekkour, 2008). CMC solutions exhibit shear-thinning behavior with a critical shear rate estimated using $1/\lambda$. Cross-model parameters obtained by rheological data fitting are presented in table S1. During injection, the applied shear rate on liquid varies from

location to location, i.e., the shear rate was different for liquid in the syringe barrel, liquid passing through the needle and liquid dispersing inside the skin.

Forcing 1% and 2% CMC solutions through a 27-gauge needle at 1 ml/min generates a high shear rate ($\sim 1.83 \times 10^4 \text{ s}^{-1}$) in the needle resulting in lower apparent viscosity, due to which the force profiles for injection in air flattened after 2 s of injection (Allmendinger et al., 2014; Rohilla et al., 2019; Benchabane and Bekkour, 2008). In the case of injections into the intradermal region, the force increased linearly for all liquids as shown in Fig. 3(d), indicating counter-pressure buildup within the tissue. Thus, the force required to inject a drug in different regions of the porcine skin depends on the morphological properties of the skin, fluid properties, needle dimensions, and variability in force required in syringe operation due to manufacturing (Rathore et al., 2012; Rathore et al., 2011). In ID injections, the stiff elastic matrix of the dermis region offered high resistance to the liquid inflow which caused the higher force required for injection, whereas moderately permeable structures of the muscular layer offer lower resistance to liquid inflow. This explains the ease of injection administration in IM injections in comparison to ID injections. To single out the contribution from tissue counter-pressure, it is necessary to subtract the reference forces (Fig. 3(a,c)) from the forces measured in tissue injections (Fig. 3(b,d)).

Fig. 4 shows the net force for liquids with different apparent viscosities. The net force for intramuscular injection via 22-gauge needle was nearly the same ($\leq 0.2 \text{ N}$) for the liquids used in the study meaning that the resistance offered by the fibrous structure of muscle tissue to the liquid inflow during injection was not significant (Zuidema et al., 1988). For intramuscular injections of Newtonian liquids, the effect of apparent viscosity on characteristic forces ($F_{B,\text{Net}}$, $F_{50\%,\text{Net}}$ and $F_{99.9\%,\text{Net}}$) was insignificant ($p > 0.05$). However, in non-Newtonian liquids, variation in apparent viscosity affected $F_{50\%,\text{Net}}$ ($p < 0.05$) significantly, whereas for net break-loose force and $F_{99.9\%,\text{Net}}$ such effect was not significant ($p > 0.05$). It is noteworthy that the break-loose force required in starting the piston motion was nearly the same for different liquids injected through a 22-gauge needle into air or intramuscular region of porcine tissue. The characteristic forces for injection into air and tissue are presented in supplementary info. Note that the negative net force observed in Fig. 4 was caused by the large variation in the measured force (for injections without any target media and in intramuscular region of the skin) and a small sample space ($n = 5$).

The net characteristic forces for intradermal injection via a 27-gauge needle for different liquids are presented in Fig. 4(b), which show a qualitatively different picture from the IM injections with substantially higher forces. The effect of apparent viscosity on net break-loose force ($F_{B,\text{Net}} = \mathcal{O}(0.1) \text{ N}$) was insignificant for intradermal injections with Newtonian and non-Newtonian liquids ($p > 0.05$). However, we can interpret the difference between the net break-loose force and the forces at 50% delivery and 99.9% delivery as the counterpressure buildup within the skin. Both of the characteristic forces ($F_{50\%,\text{Net}}$ and $F_{99.9\%,\text{Net}}$)

were higher for intradermal injections indicating high pressure buildup within the skin with time (or volume injected). It should be noted that the net forces for 50% and 99.9% delivery were higher for non-Newtonian liquids in comparison to Newtonian liquids for a similar range of apparent viscosity. Here, the apparent viscosity was estimated from the calculated shear rate in the needle, but as the liquid leaves the needle and accumulates in skin, the shear rate decreases leading to an increase in apparent viscosity. Thus, higher counterpressure buildup in the skin resulted in a higher force requirement for injecting non-Newtonian liquids. Moreover, with the increase in apparent viscosity, $F_{50\%,\text{Net}}$ and $F_{99.9\%,\text{Net}}$ decreased non-linearly for Newtonian and non-Newtonian liquids and this effect was statistically significant for both types of liquids ($p < 0.05$). Accumulation of fluid at the site of injection stretches the surrounding tissue and leads to a higher elastic response and higher counterpressure. According to the governing equations for flow in porous media (e.g. Darcy's law), increasing viscosity results in lower velocity (or flow rate) through the media. Therefore, it is counter-intuitive that the net force decreases with increasing viscosity, as seen in Fig. 4b, since this indicates that higher viscosity fluids can flow more readily away from the injection site. At present, we are unaware of other studies that have observed this trend.

3.2. Effect of volumetric flow rate

The volumetric flow rates of injections administered by health care personnel vary and can lead to different magnitudes of counterpressure buildup. Therefore, in this section of our study, we have used different flow rates of dyed water in the range of 0.1 ml/min to 2 ml/min to understand their effect on the net characteristic forces. The needle size was 22 G for IM injections and 27G for the ID injection.

Force profiles and net characteristic forces for intradermal and intramuscular injections are presented in Fig. 5; which shows a shift towards higher magnitude with the increase in volumetric flow rate as can be seen in Fig. 5(a). The inset plot in Fig. 5(a) shows the peaks in the force profiles corresponding to break-loose force, which increased with the flow rate. Break-loose force for a low flow rate of 0.1 ml/min was observed at $t \sim 0.5$ seconds, whereas for other flow rates break-loose force occurred at $t \sim 0.1$ seconds. The behavior of the force profile for variations in flow rate for intradermal injections (Fig. 5(b)) was qualitatively different than that observed in intramuscular injections as seen earlier for different liquids. Unlike intramuscular injection, the intradermal force increased linearly after the break-loose force, as shown in the inset plot in Fig. 5(b).

Net characteristic forces corresponding to break-loose force, 50% and 99.9% delivery are shown in Fig. 5(c), indicating that the net break-loose for both intradermal and intramuscular injections was very small, regardless of flow rate. $F_{50\%,\text{Net}}$ and $F_{99.9\%}$ increased non-linearly with increase in flow rate for intradermal injections, where increase in $F_{50\%}$ for $Q > 0.5 \text{ ml/min}$ was relatively small. The effect of flow rate was

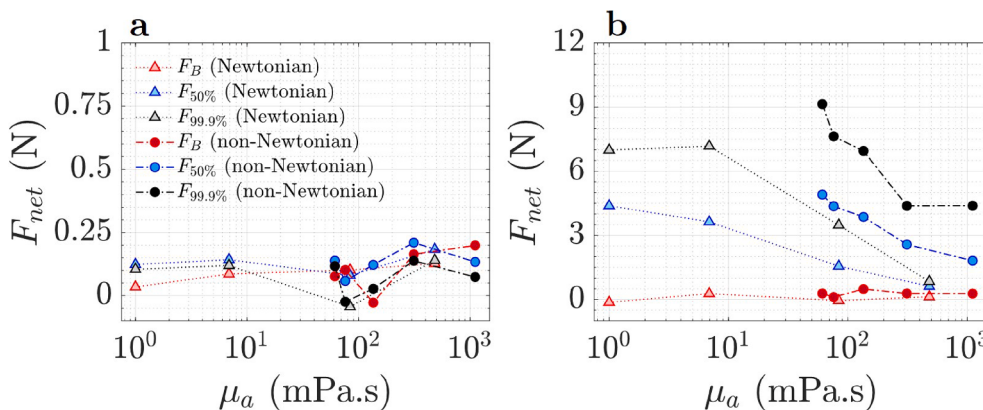


Fig. 4. Net characteristic force for Newtonian and non-Newtonian liquids. F_{Net} ($= F_{\text{tissue}} - F_{\text{air}}$) for variation in apparent viscosity of liquid injected into (a) intramuscular and (b) intradermal region of porcine skin. Legends for both subfigures are same and are presented in subfigure (a). F_{tissue} and F_{air} represent average values of 5 trials. Apparent viscosities are calculated from equation (1) corresponding to the highest shear rate as noted in Table 2. Net force values represent average values obtained from the difference of average force required to inject the liquids into air and porcine tissue.

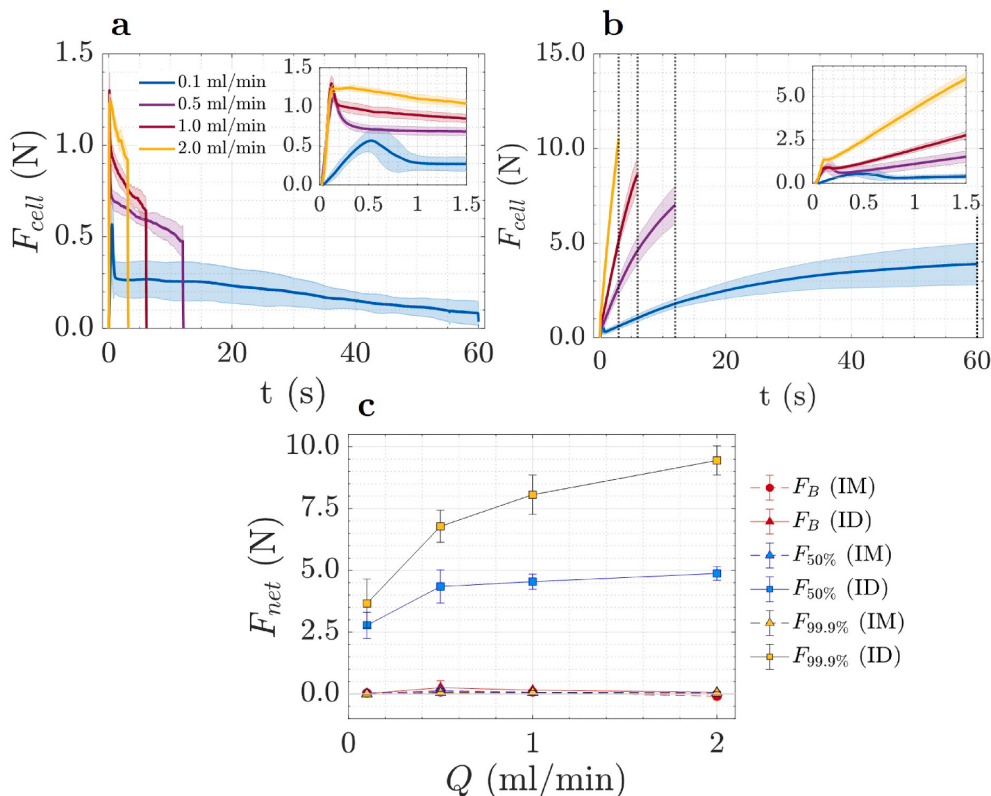


Fig. 5. Effect of volumetric flow rate of dyed water as a liquid injectate on (a) the force profile measured for IM injection (27G needle), (b) force profile for ID injection (22G needle), and (c) net force caused by counterpressure buildup in the ID and IM regions of porcine skin. (Liquid injectate: dyed water, V = 0.1 ml (ID), V = 0.5 ml (IM), n = 5, shaded and point errorbars represent the standard deviation).

insignificant on net characteristic forces ($F_{B,Net}$, $F_{50\%,Net}$ and $F_{99.9\%,Net}$) for intramuscular injections in tenderloin tissue ($p > 0.05$) and on net break-loose force ($F_{B,Net}$) for intradermal injections in porcine skin ($p > 0.05$). However, the effect of flow rate on net characteristic force at 50% and 99.9% delivery in ID injection was highly significant ($p \ll 0.05$).

3.3. Effect of needle size

The recommended needle size for intradermal injection is 27-gauge, whereas for intramuscular injection, the needle size should be in the range of 22-gauge to 25-gauge. Here, we studied the effect of three different needle sizes (22G, 25G, and 27G) to understand their effect on the counterpressure buildup during intradermal and intramuscular injections. Although 27G needles are not commonly used in intramuscular injections, we used it in our study to check their effect on counterpressure inside the tissue. The force profiles and net characteristic forces for different needle sizes are shown in Fig. 6. It should be noted that the target volume for intradermal and intramuscular injections was 0.1 ml and 0.5 ml, respectively.

For intramuscular injections, higher force was required to inject dyed water for decreasing needle size as shown in Fig. 6(a). Interestingly, there was no significant effect ($p > 0.05$) of needle size on the characteristic forces (Fig. 6(c)). Break-loose force and force measured at 50% and 99.9% delivery of the target volume was very small ($\mathcal{O}(0.1N)$), which implies the porous fibrous structure does not offer any significant resistance to the liquid inflow inside the tissue. It has been shown in the past, that the reduction of needle diameter reduces the pain associated with injection with increase in force required for liquid injection in subcutaneous tissue (Cilurzo et al., 2011; Rathore et al., 2011). The force required for intramuscular injection increased due to decreasing needle size as one can deduce from Hagen Poiseuille equation ($Re \sim \mathcal{O}(10^{-2} - 10^2)$), where $\Delta P \propto 1/r^4$. Thus, the role of tissue

properties was insignificant in counterpressure buildup during IM injection.

Fig. 6(b) shows nearly linear force measurement profiles during intradermal injection into porcine skin. Variation in needle size does not yield any substantial effect on the force profiles. Moreover, there was no significant effect of increasing needle size on the characteristic forces measured during ID injection ($p > 0.05$). Thus, the mechanical properties of the porcine dermis along with other parameters overpower the effect of needle size on the counterpressure developed within the dermal region. Although needle size showed no significant effect on counterpressure buildup, the recommended needle size for intradermal delivery should be within 25G-27G due to difficulties associated with intradermal injections with needles having larger diameter.

3.4. Effect of hyaluronidase as an adjuvant

Hyaluronidase solutions in different concentrations were used as adjuvants in dyed water (total volume injected, $V = 0.1$ ml) to understand their effect on the counterpressure buildup during injection. Viscosities of hyaluronidase solution were ~ 54.5 mPa.s and ~ 55 mPa.s for concentrations of 1 mg/ml and 2 mg/ml respectively. Fig. 7 shows the effect of hyaluronidase on the force profiles and characteristic forces during injection into different targeted regions in the skin at a flow rate of 1 ml/min. Although the addition of hyaluronidase did not show any effect on the force profiles for ID and IM injections, the force measured during SC injections decreased by nearly half. In terms of characteristic forces (F_B , $F_{50\%}$, and $F_{99.9\%}$), the effect of adding adjuvant in different concentrations was significant for SC injections ($p < 0.05$), but insignificant for IM ($p > 0.05$) and ID ($p > 0.05$) injections.

As discussed earlier, very low counterpressure was observed for IM injections due to the porous fibrous structure of the muscular layer therefore, addition of hyaluronidase does not affect the counterpressure

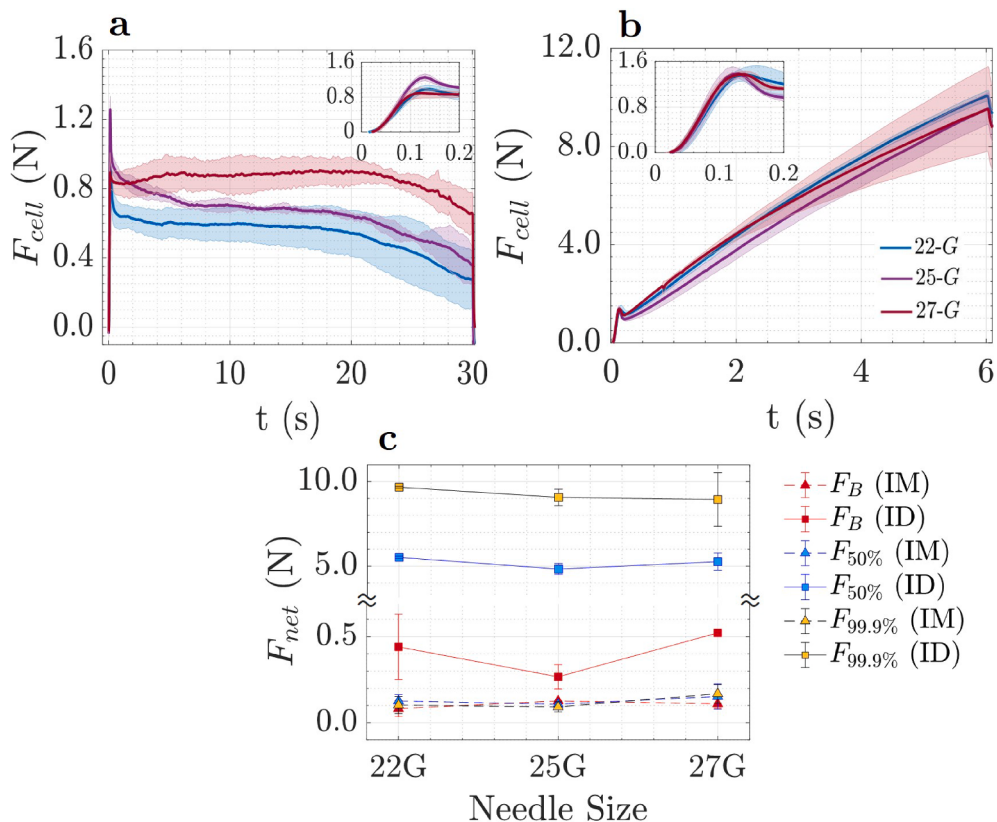


Fig. 6. Effect of needle size on (a) the force profiles for ID injections with different needle sizes and (b) characteristic forces for intramuscular injections for different needle sizes (See fig (b) for legend).(c) Net force due to tissue resistance for both ID and IM injections (Liquid injectate: dyed water, $Q = 1 \text{ ml/min}$, $V = 0.1 \text{ ml}$ (ID), $V = 0.5 \text{ ml}$ (IM), $n = 5$, shaded and point errorbars represent the standard deviation).

buildup for IM tissue. Whereas in ID injection, the addition of hyaluronidase was also insignificant, in this case due to the stiff elastic matrix of the dermis layer, which is seemingly unaffected by the hyaluronidase at the concentrations used in this study. In contrast, for SC injections, hyaluronidase increased the permeability of the cutaneous layer, which largely consists of adipose cells and thus, lowers the counterpressure buildup in addition to creating a more dispersed (wider) bolus formation as shown in Fig. 7(e). Lowering counterpressure buildup with the addition of hyaluronidase can help in alleviating pain in SC injections and can allow higher dosage of SC injections.

3.5. Counterpressure estimation

In order to estimate the magnitude of the tissue counterpressure from the recorded forces, we require an effective area; the natural choice is that of the bolus within the tissue. However, the bolus shape after injection was that of an oblate spheroid, centered at a point source (the tip of the needle) and tilted at an angle (Fig. 2(c,d)) depending on the bevel orientation. As such, we use the 2-D projected areas to convert into a spherical equivalent diameter and surface area (see Fig. S2). For consistency across each tissue type, we take the force and area for a volume of 0.1 mL. The corresponding force is calculated as follows: The total force measured during the injection consists of hydrodynamic force (F_H) inside the syringe and resistance from the tissue (F_{tissue}). Since we subtract the force measured for injection into air from the force measured during the injection in tissue, we effectively eliminated F_H . Thus, counterpressure buildup inside the tissue can be estimated using F_{net} and the equivalent spherical area of the bolus.

However, it should be noted that the bolus projected areas (Fig. S2) may also incorporate tissue imbibed with injected liquid. Furthermore, projected area for 0.1 mL injected in SC injection was three times larger than for blebs formed for ID injection. Thus, we estimated the counter

pressure in orders of magnitude. This caveat notwithstanding, we estimate the maximum pressure for IM, SC and ID tissues as $\mathcal{O}(10^{-1})$, $\mathcal{O}(10^1)$ and $\mathcal{O}(10^2)$ kPa respectively.

In the case of IM injection, the force was nearly constant with increase in the area covered by the injected liquid with time. This means that counterpressure buildup either remained constant or decreased with the liquid inflow over time due to negligible resistance offered by the muscle tissue. It should be carefully noted that the projected area does not necessarily represent the actual area occupied by the liquid injected but rather represents the area of tissue imbibed with the dyed liquid. For SC and ID injections, force measured with time during injection increased with increase in the volume of the liquid injected. However, in the absence of a direct measurement of the projected area with time, it is inconclusive to say if the change in counterpressure buildup was significant or not.

Our estimates herein show decreasing counterpressure moving away from the top layer of the skin, which is not surprising given that the outer layers of tissue (stratus corneum) are under tension. However, it is interesting to note that intradermal injections are not known to induce pain in the same way that has been documented for deeper injections. This is possibly due to the reduced volume and shallow depth for intradermal injections, meaning that fewer nerves receptors are stimulated regardless of the increased localized pressure build-up.

4. Conclusions and outlook

Characteristic forces at different times of injection were used to represent the counterpressure buildup within the skin. The net characteristic forces were small for intramuscular injections in comparison to intradermal injections due to the highly permeable and aligned fibrous structure of the muscular tissue. Higher stiffness and strong elastic

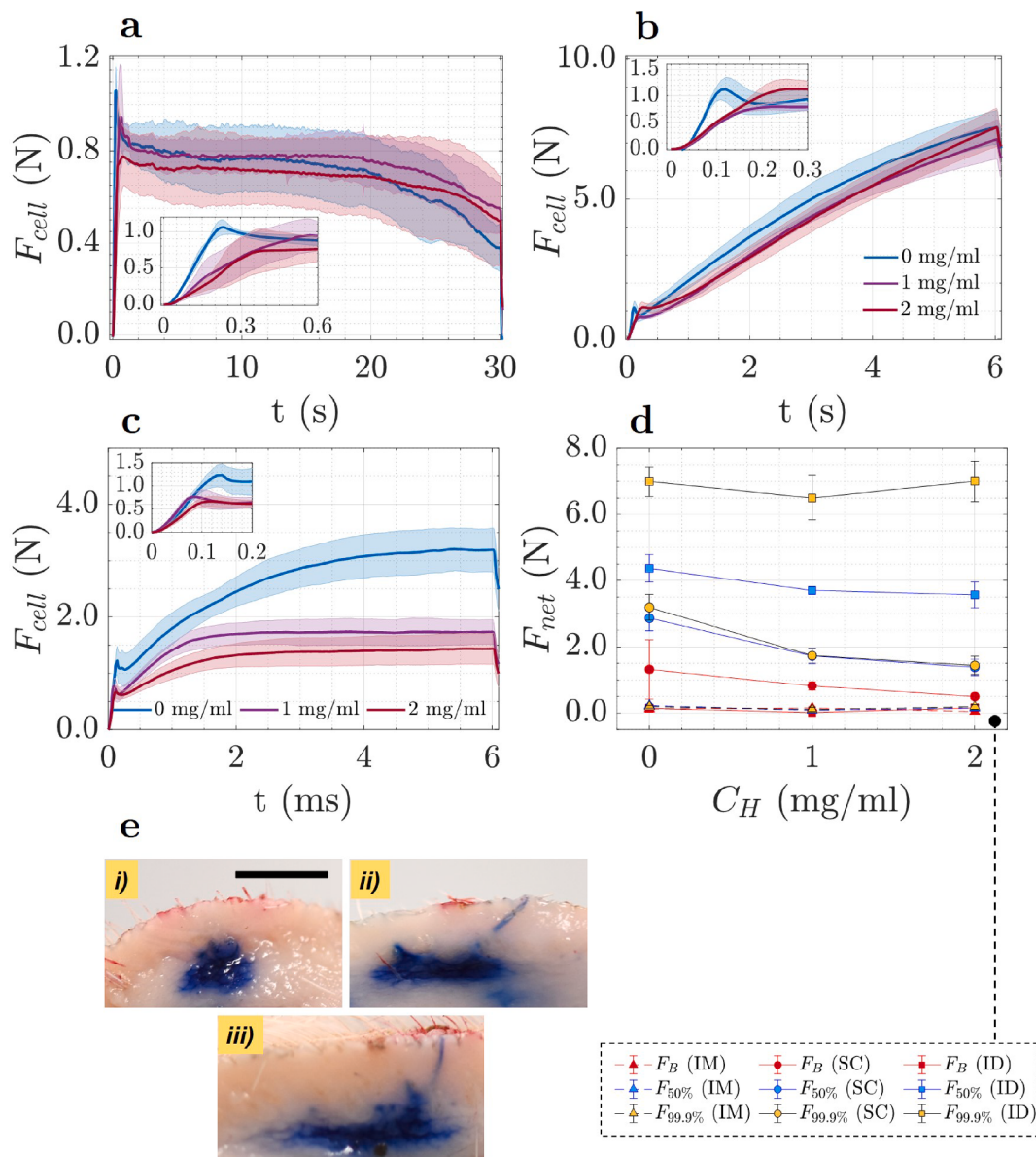


Fig. 7. Effect of hyaluronidase as an adjuvant on force profiles for (a) intramuscular injections, (b) intradermal injections, (c) subcutaneous injections, and on (d) characteristic forces for IM, SC and ID injections. (Liquid injectate: dyed water, $Q = 1 \text{ ml/min}$, $V = 0.1 \text{ ml}$ (ID, SC), 0.5 ml (IM), needle size: 22G (IM), 25G (SC) and 27G (ID), $n = 5$, shaded and point errorbars represent the standard deviation). (e) cross-sections showing the spread of liquid injectate for SC injections with different concentrations of hyaluronidase (i) 0 mg/ml, (ii) 1 mg/ml, and (iii) 2 mg/ml. (Scale bar represents 6 mm). Inset in (a-c) shows the break-loose force.

matrix in the dermal region of the skin offer higher resistance to the liquid inflow, causing higher counterpressure buildup, which could potentially limit the target volume and viscosity of a drug that can be injected intradermally. The different parameters used in the study showed an insignificant effect on the net break-loose force required to initiate the plunger motion for injection. Different liquids with varying viscosities showed a highly significant effect on $F_{50\%,Net}$ and $F_{99.9\%,Net}$ for intradermal injections, whereas for intramuscular injections, such effect was insignificant. Varying infusion rate showed a significant effect on the characteristic forces during ID injection with no significant effect in IM injections. Moreover, adding an adjuvant only helped in decreasing counterpressure buildup in SC injections with no significant effect in ID and IM injections. Thus, adjuvants can be used to facilitate the administration of higher doses of SC injection with wider dispersion within the cutaneous tissue. As the porcine skin is the closest model of human skin, results in this study for porcine skin and tissue used after a cycle of freezing and thawing, which can be translated to injections in human

tissue. The results obtained here in this ex vivo study could be helpful in designing injectors to minimize higher counterpressure buildup and an in vivo study could provide more insight into the counterpressure buildup. One interesting observation from our study was that the net force for intradermal injections decreased as the liquid viscosity increased. We are unaware of any other studies which have reported this seemingly counter-intuitive result.

CRediT authorship contribution statement

Md Shahriar: Data curation, Writing - original draft. **Ankit Rewanwar:** Data curation, Formal analysis. **Pankaj Rohilla:** Methodology, Data curation, Writing - original draft, Writing - review & editing. **Jeremy Marston:** Conceptualization, Methodology, Writing – review & editing, Funding acquisition.

Declaration of Competing Interest

The authors declare that they have no known competing financial interests or personal relationships that could have appeared to influence the work reported in this paper.

Acknowledgments

J.M. acknowledges funding support through NSF (CAREER award No. 1749382).

Appendix A. Supplementary material

Supplementary data associated with this article can be found, in the online version, at <https://doi.org/10.1016/j.ijpharm.2021.120530>.

References

- Allmendinger, Andrea, Fischer, Stefan, Huwyler, Joerg, Mahler, Hanns-Christian, Schwarb, Edward, Zarraga, Isidro E., Mueller, Robert, 2014. Rheological characterization and injection forces of concentrated protein formulations: an alternative predictive model for non-newtonian solutions. *Eur. J. Pharmaceut. Biopharmaceut.* 87 (2), 318–328.
- Allmendinger, Andrea, Mueller, Robert, Schwarb, Edward, Chipperfield, Mark, Huwyler, Joerg, Mahler, Hanns-Christian, Fischer, Stefan, 2015. Measuring tissue back-pressure-in vivo injection forces during subcutaneous injection. *Pharmaceut. Res.* 32 (7), 2229–2240.
- Benchabane, Adel, Bekkour, Karim, 2008. Rheological properties of carboxymethyl cellulose (cmc) solutions. *Colloid Polym. Sci.* 286 (10), 1173.
- Buhren, Bettina Alexandra, Schrumpf, Holger, Hoff, Norman-Philipp, Bölké, Edwin, Hilton, Said, Gerber, Peter Arne, 2016. Hyaluronidase: from clinical applications to molecular and cellular mechanisms. *Eur. J. Med. Res.* 21 (1), 5.
- Burckbuchler, V., Mekhloufi, G., Paillard Giteau, A., Grossiord, J.L., Huille, S., Agnely, F., 2010. Rheological and syringeability properties of highly concentrated human polyclonal immunoglobulin solutions. *Eur. J. Pharmaceut. Biopharmaceut.* 76 (3), 351–356.
- Cavallini, Maurizio, Gazzola, Riccardo, Metalla, Marco, Vaienti, Luca, 2013. The role of hyaluronidase in the treatment of complications from hyaluronic acid dermal fillers. *Aesthetic Surg. J.* 33 (8), 1167–1174.
- Cilurzo, Francesco, Selmin, Francesca, Minghetti, Paola, Adamo, Marco, Bertoni, Elisa, Lauria, Sara, Montanari, Luisa, 2011. Injectability evaluation: an open issue. *AAPS PharmSciTech* 12 (2), 604–609.
- Comley, Kerstin, Fleck, Norman, 2011. Deep penetration and liquid injection into adipose tissue. *J. Mech. Mater. Struct.* 6 (1), 127–140.
- Cross, Malcolm M., 1965. Rheology of non-newtonian fluids: a new flow equation for pseudoplastic systems. *J. Colloid Sci.* 20 (5), 417–437.
- El-Safory, Nermene S., Fazary, Ahmed E., Lee, Cheng-Kang, 2010. Hyaluronidases, a group of glycosidases: Current and future perspectives. *Carbohydr. Polym.* 81 (2), 165–181.
- Harris, Reed J., Shire, Steven J., Winter, Charles, 2004. Commercial manufacturing scale formulation and analytical characterization of therapeutic recombinant antibodies. *Drug Develop. Res.* 61 (3), 137–154.
- Kim, Hyejeong, Park, Hanwook, Lee, Sang Joon, 2017. Effective method for drug injection into subcutaneous tissue. *Sci. Rep.* 7 (1), 1–11.
- Leuenberger, James P., Jockel, Philipp Roebrock, Shergold, Oliver A., 2013. Insulin depot formation in subcutaneous tissue. *Journal of Diabetes. Sci. Technol.* 7 (1), 227–237.
- Lorenz, B., Krick, B.A., Rodriguez, N., Sawyer, W.G., Mangiagalli, P., Persson, B.N.J., 2013. Static or breakloose friction for lubricated contacts: the role of surface roughness and dewetting. *J. Phys.: Condens. Matter* 25 (44), 445013.
- McDonald, Thomas A., Zepeda, Monica L., Tomlinson, Michael J., Bee, Walter H., Ivens, Inge A., 2010. Subcutaneous administration of biotherapeutics: current experience in animal models. *Curr. Opin. Mol. Ther.* 12 (4), 461–470.
- Meyer, Karl, 1947. The biological significance of hyaluronic acid and hyaluronidase. *Physiol. Rev.* 27 (3), 335–359.
- Patte, Caroline, Pleus, Stefan, Wiegel, Chris, Schiltges, Gilbert, Jendrike, Nina, Haug, Cornelia, Freckmann, Guido, 2013. Effect of infusion rate and indwelling time on tissue resistance pressure in small-volume subcutaneous infusion like in continuous subcutaneous insulin infusion. *Diabetes Technol. Therapeut.* 15 (4), 289–294.
- Pivot, Xavier, Gligorov, Joseph, Müller, Volkmar, Barrett-Lee, Peter, Verma, Sunil, Knoop, Ann, Curigliano, Giuseppe, Semiglavov, Vladimir, López-Vivanco, Guillermo, Jenkins, Valerie, et al., 2013. Preference for subcutaneous or intravenous administration of trastuzumab in patients with her2-positive early breast cancer (prefer): an open-label randomised study. *Lancet Oncol.* 14 (10), 962–970.
- Pstrasz, Leszek, 2016. Valsalva manoeuvre using a syringe: physics and implications. *Emerg. Med. J.* 33 (11), 831.
- Rathore, Nitin, Pranay, Pratik, Eu, Bruce, Ji, Wenchang, Walls, Ed, 2011. Variability in syringe components and its impact on functionality of delivery systems. *PDA J. Pharmaceut. Sci. Technol.* 65 (5), 468–480.
- Rathore, Nitin, Pranay, Pratik, Bernacki, Joseph, Eu, Bruce, Ji, Wenchang, Walls, Ed, 2012. Characterization of protein rheology and delivery forces for combination products. *J. Pharmaceut. Sci.* 101 (12), 4472–4480.
- Richter, Wolfgang F., Bhangali, Suraj G., Morris, Marilyn E., 2012. Mechanistic determinants of biotherapeutics absorption following sc administration. *AAPS J.* 14 (3), 559–570.
- Rohilla, Pankaj, Rane, Yatish S., Lawal, Idera, Le-Blanc, Andrew, Davis, Justin, Thomas, James B., Weeks, Cormak, Tran, Whitney, Fisher, Paul, Broderick, Kate E., Simmons, Jonathan A., Marston, Jeremy O., 2019. Characterization of jets for impulsively-started needle-free jet injectors: Influence of fluid properties. *J. Drug Deliv. Sci. Technol.* 53, 101167.
- Saitoh, Akihiko, Aizawa, Yuta, 2016. Intradermal vaccination for infants and children. *Human Vaccines Immunotherapeut.* 12 (9), 2447–2455.
- Salari, Maryam, Estaji, Zahra, Akrami, Rahim, Rad, Mostafa, 2018. Comparison of skin traction, pressure, and rapid muscle release with conventional method on intramuscular injection pain: A randomized clinical trial. *J. Educat. Health Promot.* 7.
- Shrestha, Pranav, Stoeber, Boris, 2018. Fluid absorption by skin tissue during intradermal injections through hollow microneedles. *Sci. Rep.* 8 (1), 1–13.
- Thomsen, Maria, Hernandez-Garcia, Anier, Mathiesen, Joachim, Poulsen, Mette, Sørensen, Dan N., Tarnow, Lise, Feidenhans, Robert, 2014. Model study of the pressure build-up during subcutaneous injection. *PLoS One* 9 (8).
- Thomsen, Maria, Rasmussen, Christian Hove, Refsgaard, Hanne H.F., Pedersen, Karen-Margrethe, Kirk, Rikke K., Poulsen, Mette, Feidenhans, Robert, 2015. Spatial distribution of soluble insulin in pig subcutaneous tissue: effect of needle length, injection speed and injected volume. *Eur. J. Pharm. Sci.* 79, 96–101.
- Thornton, Hilary Sarah, Elwan, Mohammed H., Reynolds, Joseph A., Coats, Timothy J., 2016. Valsalva using a syringe: pressure and variation. *Emergency Med. J.* 33 (10), 748–749.
- Tuğrul, Emel, Khorshid, Leyla, 2014. Effect on pain intensity of injection sites and speed of injection associated with intramuscular penicillin. *Int. J. Nursing Practice* 20 (5), 468–474.
- Vosseler, Michael, Jugl, Michael, Zengerle, Roland, 2011. A smart interface for reliable intradermal injection and infusion of high and low viscosity solutions. *Pharmaceut. Res.* 28 (3), 647–661.
- Wangmo, Karma, Laven, Richard, Cliquet, Florence, Wasniewski, Marine, Yang, Aaron, 2019. Comparison of antibody titres between intradermal and intramuscular rabies vaccination using inactivated vaccine in cattle in bhutan. *PLoS One* 14 (6), e0209946.
- Wynaden, Dianne, Tohotoa, Jenny, Omar, A.L., Happell, Brenda, Heslop, Karen, Barr, Lesley, Sourinathan, Vijay, 2015. Administering intramuscular injections: How does research translate into practice over time in the mental health setting? *Nurse Education Today* 35 (4), 620–624.
- Yıldız, Arda, Lenau, Torben Anker, 2019. In vitro simulation of tissue back-pressure for pen injectors and auto-injectors. *J. Pharmaceut. Sci.* 108 (8), 2685–2689.
- Zuidema, J., Pieters, F.A.J.M., Duchateau, G.S.M.J.E., 1988. Release and absorption rate aspects of intramuscularly injected pharmaceuticals. *Int. J. Pharmaceut.* 47 (1–3), 1–12.